Supplementary Data

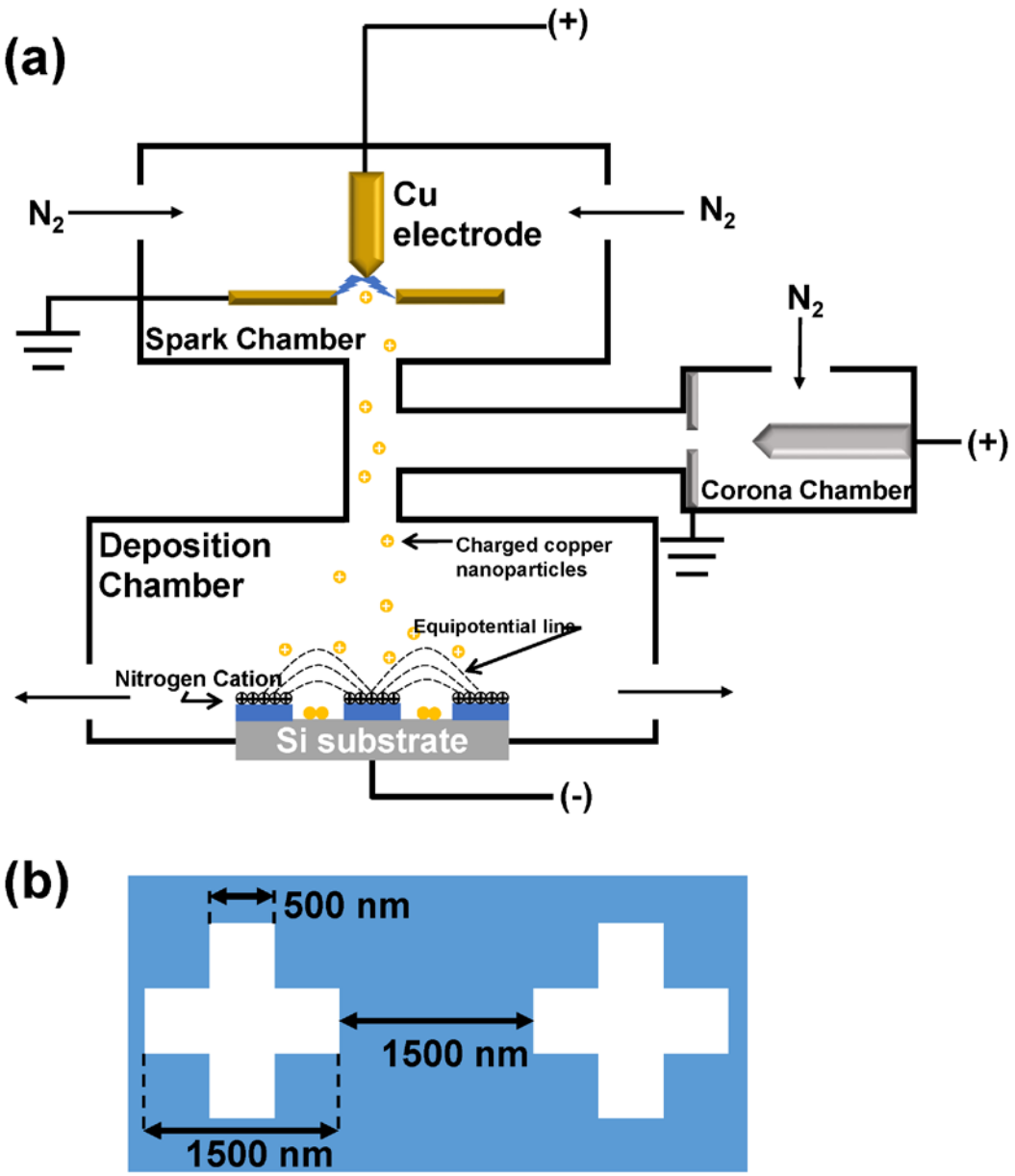

Figure S1. (a) Experimental set-up scheme for ion-assisted aerosol lithography (IAAL). Positively charged nitrogen ions and copper nanoparticles are generated from corona chamber and spark chamber, respectively and deposited at the substrate in deposition chamber. (b) The square cross-shape pattern of resist layer used for nano-assemblty via IAAL.

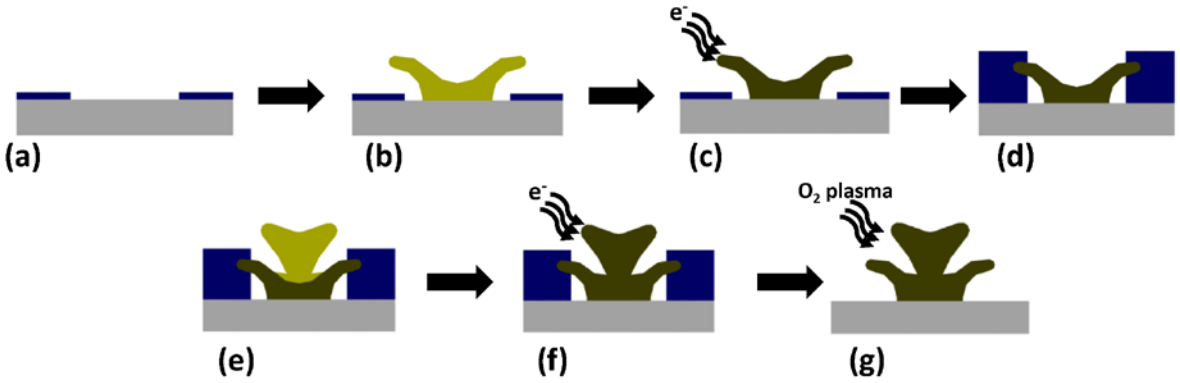

Figure S2. Cross-sectional view of schematics for stacking 3D nanostructures (a) Preparation of resist patterns. (b) Fabrication of 3D nanostructures via IAAL. (c) Sintering nanostructures via electron beam irradiation. (d) Preparation of another patterns for the upper nanostructures after spin-coating the resist. (e) Fabrication of the upper nanostructures. (f) Sintering nanostructures. (g) Removal of the resist.

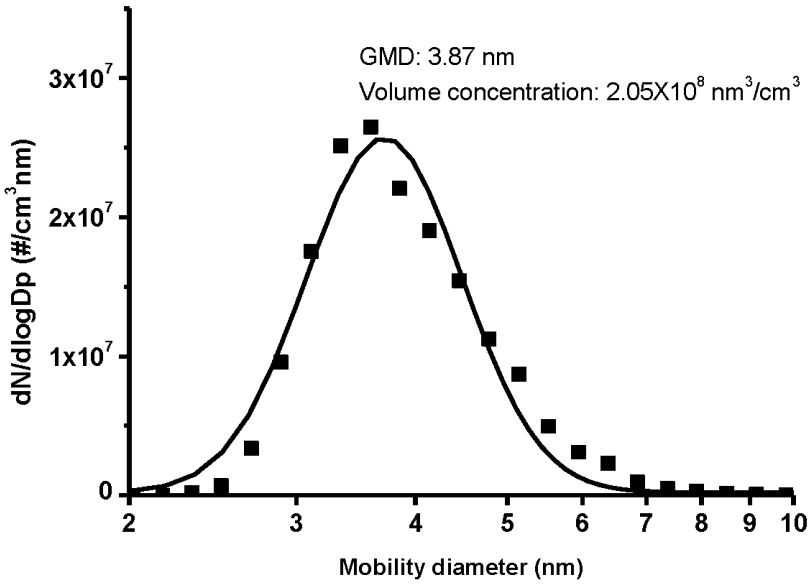

Figure S3. Particle size distribution measured by scanning mobility particle sizer (SMPS) system. Geometric mean diameter is measured as 3.87 nm and volume concentration is measured as 2.05×10^8 nm^3/cm^3, respectively.

Table S1. SERS peak intensities at 1575 cm-1 of five different spots in two different samples for mono-layer 3D nanostructures and bi-layer 3D nanostructures

Sample Name	SERS peak intensity at 1575 cm^{-1} (a.u.)						
	1	2	3	4	5	Average	Standard deviation
Mono-layer Sample #1	2322	2332	2502	2885	2205	2329	97
Mono-layer Sample #2	2257	2090	2330	2231	2305	2242	94
Bi-layer Sample #1	10425	11639	10708	10768	9839	10676	652
Bi-layer Sample #2	10091	9620	10322	10188	9521	9948	356

Table S2. SERS peak intensities at 1575 cm-1 of five different spots in each sample with various values of r

r	deposition time (min)	1	2	3	4	5	Average	Standard deviation
0.35	5	2596	2983	2357	2535	2541	2602	231
0.42	10	6801	6447	6448	6126	7040	6581	351
0.48	20	8873	9436	8881	8624	8415	8846	383
0.5	20	11163	9514	9943	10902	9128	10130	877
0.53	30	12230	14013	12190	12037	10322	12158	1307
0.55	30	11152	11474	11005	11836	9891	11071	733
0.6	40	10091	9620	9203	9159	9521	9519	376
0.63	40	8729	8680	8270	8427	8572	8536	188
0.68	50	5454	6381	5152	6062	6758	5962	658
0.75	50	4383	4497	4313	4366	4221	4356	101
1	60	2485	2540	2410	2834	2686	2591	169

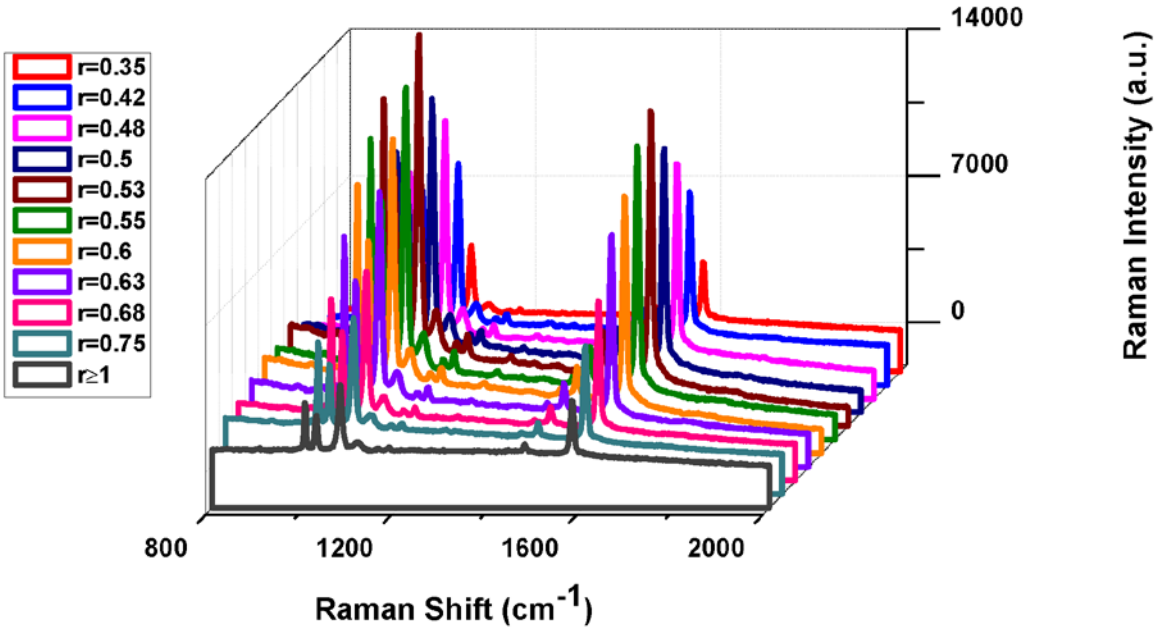

Figure S4. Raman spectra of various values of r